Modelling heat and degree of gelation for methyl cellulose hydrogels with NaCl additives

S. C. Joshi[*] *and Y. C. Lam*
School of Mechanical and Aerospace Engineering
Nanyang Technological University
Singapore, 639 798.

[*] Author for correspondence: E-mail: mscjoshi@ntu.edu.sg, Phone: (65) 6790 5954, Fax: (65) 6791 1859.

[*] Author for correspondence: E-mail: mscjoshi@ntu.edu.sg, Phone: (65) 6790 5954, Fax: (65) 6791 1859.

Abstract

Methyl cellulose (MC) hydrogels are thermo reversible physical hydrogels and their gelation is endothermic. A model consisting of a general mathematical expression (for bell-shape curves) is formulated to describe and capture the enthalpy changes that take place during gelation of an aqueous solution of MC, SM 4000, in the presence of different concentrations of sodium chloride, NaCl. The constants for the mathematical expression were obtained based on calorimetric measurements. The model could describe the salt-out effects of NaCl very well.

It was noticed that more than one bell-shape curves as defined by the expression, one major and one minor, were necessary to depict the enthalpy changes appropriately. It was hypothesized that the major curve is associated with the major enthalpy change related to hydrophobic association of MC groups leading to the development of a gel network and its swelling. The minor curve describes the minor enthalpy change, which include primarily the ionic interaction of salts with water, water-to-water and water-to-polymer hydrogen bonding and energy associated in stabilizing the gel network. Subsequently, an analytical model for the degree of gelation was introduced and its development discussed to study further the effects of various salt concentrations on the gelation of MC.

1. Introduction

Hydrogels are cross-linked networks of hydrophilic/ hydrophobic polymers which are formed either by chemical or physical bonds in water. They possess the ability to absorb large amounts of water and swell while maintaining their three-dimensional structure.

Hydrogels are increasingly being used in biomedical, food and pharmaceutical industries. Most hydrogels undergo transformation from solution to gel form (commonly termed as gelation process) upon either cooling or heating. Such thermo-sensitive hydrogels are gaining more importance and being explored as media for controlled drug release [1-4].

Methyl cellulose (MC), which is extensively used as a thickener or binder in pharmaceutical, ceramic processing and food applications, undergoes gelation in aqueous solution upon heating [5-7]. Gelation of MC has been a key area of research and a clear and complete picture of the gelation mechanism has not yet been established. The sol-gel transformation process for MC, as illustrated in Figure 1, is based on various explanations provided by other researchers [5-8] and our earlier studies [9-10]. According to Kobayashi et al. [8], at low temperatures, water molecules surround the hydrophobic methaxyl groups of MC, so that MC becomes water-soluble (Figure 1a). However, upon heating, these surrounding water structures deform and break to expose the hydrophobic regions of MC (Figure 1b). Because of hydrophobic nature of these side groups, the MC chains in the aqueous solution move towards each other, bringing side groups together to associate, and form aggregates or inter-chain clusters (Figure 1c). As temperature rises further, more and more hydrophobic aggregates are formed. Eventually these aggregates join together through the hydrophobic groups developing into a three-dimensional

physical network of MC chains (Figures 1d-1f). Even when the network is fully developed, the MC mers are still in a relaxed state rendering the network cells flexible. Gradually, as temperature increases, water uptake and entrapment of water molecules into these network cells increases resulting in enlargement of these cells to full-size reducing their flexibility (Figures 1g-1h). The continued swelling of the network of MC chains is due to osmotic forces, which are opposed by the elastic retraction forces of the network. Eventually an equilibrium swelling level is attained [11] resulting into a fully developed and stabilized MC gel (Figure 1i).

As such, the sol-gel transformation of MC in an aqueous solution is distinctively marked by two processes namely, formation of MC chain network and swelling or expansion of the various cells in the network resulting into a fully developed gel. Both these transformations are linked to the absorption and utilization of heat energy, generally referred to as the heat of gelation. Differential scanning calorimeter (DSC) measurements have been successfully used to obtain quantitative information about the heat of gelation [6, 12].

Kundu and Kundu [13] investigated the effect of sodium chloride, NaCl, when added to aqueous solutions of MC, with the MC content below 1%, on the DSC measurements. It was observed that the temperature at which absorption of heat was at the peak decreased with increasing salt concentration. This is an important salt-out phenomenon that can be used to alter the sol-gel transition process to suit particular application. Xu et al. [14-15] also carried out DSC measurements on MC solutions in the presence of NaCl in order to understand the salt-out mechanism further. Newer inventions are seen where MC is modified to match their salt-out effects at body temperature [16].

The current work focuses on the modeling of the changes in enthalpy associated with the gel formation process for MC with NaCl additives at different concentration. Unless such models are available, various applications of MC hydrogels, including drug delivery and drug release, can not be systematically analyzed, understood, and improved. In our earlier work [9-10] a generalized formulation was developed and validated for modeling MC gelation. The same formulation is now modified and extended further to capture the salt effects. The necessary parameters in the formulation were determined such that close agreement was established with the DSC heating thermograms. During the model formation, it was noticed that more than one bell-shape curves, one major and one minor, were necessary to depict the enthalpy changes adequately. It was hypothesized that the major curve was related to major enthalpy change associated with the movement of MC chains, formation of MC aggregates, and hydrophobic association of MC groups finally leading to the development of a three-dimensional gel network and its subsequent swelling. The term swelling is used to highlight the enlargement of MC network cells due to uptake and entrapment of water molecules into them. The minor curve was associated with minor enthalpy change primarily involving the ionic interaction of the salts with water, water-to-water and water-to-polymer hydrogen bonding and energy associated in stabilizing the swollen gel network. Subsequently, an analytical model for the degree of gelation was introduced and its development discussed to study the effects of various concentrations of NaCl on the gelation of MC further.

2. Materials and Experimental Data

The DSC data, i.e. the relative thermal capacity, C_p, was acquired [14-15] using a micro differential scanning calorimeter (VP-μDSC, MicroCal Inc.) for the aqueous solutions of 0.03mM (0.93wt%) of MC with different % of NaCl, namely 0.2M, 0.4M, 0.6M, and 0.8M. De-ionized water was taken as a reference during the heating process at the rate of 1 °C/min. Methylcellulose, with the trade name, SM4000, was provided by Shinetsu Chemical Co. Ltd. It has a weight-average molecular weight (M_w) of 310,000 g/mol and an average degree of substitution (DS) of 1.8. NaCl was purchased from Sino Chemical Co. (Pte) Ltd.

The DSC results for the MC-NaCl solutions as documented and discussed in [14-15] were used in the present work to demonstrate the development and validity of the models. It was observed that the baseline C_p values in all cases showed small fluctuations around zero due to the initial unsteady state of the solutions and the temperature conditions before the DSC measurements attained a steady trend. As the magnitude of the base C_p value was insignificant, its small fluctuation would have little effect. As such, for convenience, a single base C_p value, set at 1×10^{-4} KJ/mol/^{o}C, was used to normalize the experimental data as depicted in Figure 2. The plots indicated that the addition of salt had an effect on the onset (T_{on}), peak (T_p), and offset (T_{off}) temperatures for the sol-gel transformation.

3. Model Development and Implementation

It was observed that most of the heating thermograms for gelation of MC hydrogels were un-symmetrical and bell-shaped (Figure 2), which required a generalized mathematical formulation to represent them. One such formulation (equation 1) was established earlier by the authors [9-10]:

$$C_p(T-T_p) = \frac{NR}{DR_1 + DR_2} = \frac{(\lambda_1 + \lambda_2)C_{p\max}}{\lambda_1 e^{(T-Tp)C_1} + \lambda_2 e^{-(T-Tp)C_2}} \quad (1)$$

where $C_p(T-T_p)$ refers to the thermal function of the specific heat capacity, NR signifies the numerator term, and DR1 and DR2 designate part 1 and part 2 of the denominator. λ_1, λ_2, C_1, and C_2 are the empirical constants which are to be determined by minimizing the discrepancy between the experimental data (DSC thermogram) and the mathematical formulation (equation 1).

There are a few similarities in the thermal behavior of hydrogels [9-10] and other polymers [17-18]. Crystallization of thermoplastics, curing of thermosetting resins and gelation of hydrogels are all governed by thermodynamic considerations. Crystallization and curing are exothermic reactions whereas gelation, depending on the type of hydrogel, can be either endothermic or exothermic process. Both crystallization and physical gelation are thermo-reversible processes. Thermosetting resins and hydrogels both have three-dimensional networks. Therefore, the term 'degree of gelation' (α_g), similar to the degree of cure or the degree of crystallization, was introduced for quantitative assessment of the state of gelation [9-10]. Once the DSC data is mapped, α_g at temperature T can be calculated as:

$$\alpha_g = \frac{\text{Heat absorbed upto a stage}}{\text{Heat for complete gelation}} = \frac{H}{H_T} = \frac{\int_{T_{on}}^{T} f(T)dT}{\int_{T_{on}}^{T_{off}} f(T)dT} \quad (2)$$

Note that α_g is a fraction that varies from 0 to 1 and is dimensionless. $\alpha_g = 0$ at $T = T_{on}$ and when $T = T_{off}$, $\alpha_g = 1$. Equations 1 and 2 were successfully used to describe the DSC heating thermograms and to obtain the heat of gelation, the degree of gelation and the swell initiation points for MC solutions of different concentrations without any additives [10]. The significance of the various constants was yet to be elaborated and will now be discussed.

From equation 1, NR is a multiplier that is determined based on the scaling requirement for *1/(DR1+DR2)*. The denominator terms control the spread and the shape of the C_p curve. *DR1* describes the decaying arm from T_p and T_{off} whereas *DR2* maps the growing arm from T_{on} to T_p. Both, *DR1* and *DR2*, have a form similar to the Arrhenius equation [19] describing the progress of a reaction as a function of temperature with time. Thus the associated constants could have similar significance. λ_1 and λ_2 are the frequency parameters with the unit *1/°C*. The terms C_1 and C_2 resemble $R/\Delta E$, where ΔE is the activation energy (J/mol) and *R* the universal gas constant (8.314 J/mol.K). Since gelation takes place only within a certain temperature window when the temperature is allowed to increase at a certain rate, the temperature difference holds the key for the reaction. Under isothermal conditions or at slow rate of heating, the gelation process appears to attain equilibrium rapidly with no further change in the state of gelation. This suggests that for a reasonably slow scan rate of 1 °C/min the temperature difference and not the duration of

the temperature change is the important parameter for gelation modeling. It was therefore possible to establish a model based on the usual temperature unit ^{o}C. The units of C_1 and C_2 in the current case thus remain as $1/^{o}C$, which cancel out with the temperature units for $(T-T_p)$ terms. *DR1* and *DR2* will have the same unit as the λ terms. Finally, $C_p(T-T_p)$ would have the same unit as that of C_{pmax} (J/mol^{o}C) as required.

Equations 1 and 2 were first used to describe the C_p values and α_g for MC solutions with 0.2M and 0.8M NaCl. The comparison between the model and the experimental data are shown in Figure 3. It is observed from these plots that the basic model, namely equation 1, could not describe the process well around the shoulders of the C_p curves. Rather large discrepancies between the model and the experimental data manifested themselves at the beginning and towards the end of gelation. These differences were reflected for the degree of gelation curves also. It is observed that the discrepancies increased with increasing NaCl concentration. Thus the model, which reasonably predicted the gelation process for MC without salt, was unable to describe the heat absorption mechanism successfully for sol-gel transformations for aqueous solution of MC in the presence of NaCl.

These discrepancies suggest that there could be additional mechanisms taking place due to the addition of NaCl. By hypothesizing that these additional mechanisms follow a similar trend for the rate of energy absorption, and that the effects of more than one binding process and mechanism can be superimposed, an expression similar to equation 1 can be added to describe these mechanisms. Thus, in order to account for the effects of

the salt additive, a model that consisted of two expressions, with each similar to that of equation 1, was employed; see equation 3.

$$C_p(T-T_p)=\frac{(\lambda_1+\lambda_2)C_{pv1}}{\lambda_1 e^{(T-T_{p1})C1}+\lambda_2 e^{-(T-T_{p1})C2}}+\frac{(\lambda_3+\lambda_4)C_{pv2}}{\lambda_3 e^{(T-T_{p2})C3}+\lambda_4 e^{-(T-T_{p2})C4}} \quad (3)$$

Where $\lambda_1, \lambda_2, \lambda_3, \lambda_4, C_1, C_2, C_3$ and C_4 are the empirical constants. Note that C_{pmax} and T_p used in equation 1 are replaced by C_{pv1}, T_{p1}, C_{pv2} and T_{p2} in equation 3. This two-expression model was expected to provide two bell-shape curves, which when superimposed, would closely follow the experimental DSC curves.

The constants for the equation could be determined by minimizing the discrepancies between the model (equation 3) and experimental data. The least square technique was adopted in which the values of the constants were obtained by iteratively minimizing the sum of square of errors in C_p values calculated as:

$$\sum_{i=1}^{N}\left[C_{p(\exp t)}-\left(C_{p1(\mathrm{mod}el)}+C_{p2(\mathrm{mod}el)}\right)\right]^2 \to 0 \quad (4)$$

where, $i = 1$ at $T = T_{on}$ and $i = N$ when $T = T_{off}$. This generated two bell-shape curves with C_{p1} and C_{p2} as their respective peak C_p values.

4.0 Results and Discussions

Figure 4 shows the heat capacity curves obtained using the model (equation 3) and its comparison with the DSC thermogram data for different concentrations of NaCl. The empirical constants for the model are listed in Table 1.

As NaCl is an electrolyte, the Cl^- ions compete with the MC chains for hydrogen (H) bonding with water molecules, which promotes early exposure of hydrophobic groups and rapid formation of MC aggregates at lower temperature. This, in turn, results in a lower T_p that decreases monotonically with an increase in salt concentration [14].

All the curves exhibited the trend that the dominant or major bell-shape curves was always able to map most of the experimental data and was designated as the primary curve. The secondary curve, which always appeared small, however, was necessary to provide good fit to the left- and right-hand shoulders of the curve. As mentioned earlier, the low temperature activities are dominated by water-to-water and water-to-MC hydrogen bonding. The low-magnitude, initial portion of the primary curve describes the energy consumption causing disruption of these bonding processes. In a similar manner and in small magnitude also, the ionic interaction of salts with water, which is also through H bonding, is represented by the initial portion of the secondary curve. This reflects that such H bonding does not involve substantial amount of energy.

Following the breakage of water-cages surrounding the hydrophobic side groups of MC chains, these chains tend to move towards each other for association. However, these macromolecules of MC are considerably long in comparison with the molecules of NaCl and H_2O. It is expected that a substantial amount of energy is required to facilitate their movement in the solution. This justifies the substantial and fast rise in C_p. As the MC molecules come closer, they start to form groups through a few hydrophobic bonds. These groups further join together and start to form a network. This initial phase of hydrophobic association is referred to as non-cooperative association and requires more

energy as compared to the subsequent bonding. The subsequent hydrophobic association occurs among the already connected MC chains thereby increasing the density of the network cells. This type of bonding requires much less energy and called as cooperative association. As long as the process of non-operative association goes on, the energy absorption continues at high rate, marked by C_p reaching C_{pv1}. It is anticipated that the cooperative association will go on for some more time until the network develops into a full three-dimensional structure. However, this stage has a much subsided energy requirement and the C_p value starts to recede. Gradually, as temperature increases, the network cells start to take in more water molecules and hold them within. Because of this expansion or swelling of the cells and reduction in their flexibility, the gel starts to exhibit higher and higher elastic properties.

The peak of the second curve shifted towards the right indicating increased energy utilization with salt additives during the swelling of the gel network and the gel stabilization phase. The gradual shift of the peak to the right and the increase in the magnitude of C_{pv2} with higher NaCl concentration may be attributed to the increasing interaction between the salt ions and water molecules that delayed water molecules from entering the orderly state within the gel network. This is evident from Figure 4 for all NaCl concentrations. As the salt concentration increased, higher C_{pv2} values were observed indicating a rise in the heat energy absorbed. With additional interactions between the salt ions and the water molecules, the total enthalpy change, H_T, was higher for higher NaCl concentrations. It is evident from Figure 5 that H_T values increased linearly with NaCl concentration. The trend-line as depicted by equation 5 shows that an additional energy of 1067.64 kJ was required per 0.2M/mol of NaCl.

$$H_T \text{ (kJ/mol)} = 3815.7 + 5338.2 * (NaCl \text{ Concentration in M}) \quad (5)$$

However, it could not be ascertained whether the original energy requirement for MC reduced in the presence of the salt.

The plots of the degree of gelation versus temperature for all NaCl concentrations (determined using equation 2) are shown in Figure 6. The α_g curves approximately have the same slope between $\alpha_g \approx 0.1$ and 0.6. This implies that the rate of gelation was not affected by the presence of NaCl during this phase. This was the window when the MC macromolecules were moving closer and the development of the gel network was in progress.

It is evident that the formulation presented in equation 3 could describe the energy utilization for MC gelation in the presence of NaCl. However, no specific trend for the various constants listed in Table 1 was observed. One of the primary reasons might be the mechanism and the transformations instigated by a specific amount of NaCl salt added to MC solution. Although the total heat of gelation appeared to follow a linear growth with salt concentration (Figure 5), the internal mechanisms may not be sharing the energy in the same proportion.

5.0 Sigmoidal Model for Degree of Gelation Curves

Being a representation of a transformation process in a bio-polymeric material, the degree of gelation curves are rather similar to the degree of cure curves for thermosetting polymers [20] and degree of crystallization curves for thermoplastics [21]. The difference is that gelation of MC is driven predominantly by the change of temperature, and the time

parameter is of little significance. As such, one could map α_g curves directly instead of trying to model the rate of change in α_g. A good candidate is the sigmoidal curve of the logistics curves family. It is known to describe 'S' curves well and has been used for biomedical and biomaterials related studies [22-23]. The following sigmoidal growth curve (equation 6) was found to describe α_g curves very well for gelation of MC with NaCl additive.

$$\alpha_g(T-T_p)=\left(\frac{T-T_{on}}{T_{off}-T_{on}}\right)\frac{\psi_1+\xi_1 e^{(T-T_p)B_1}}{\psi_2+\xi_2 e^{(T-T_p)B_2}} \tag{6}$$

Note that six empirical constants were employed in an unconstrained manner deliberately to avoid an over-constrained equation that could result in poor data fitting. $\left(\frac{T-T_{on}}{T_{off}-T_{on}}\right)$ is a temperature range fraction to enforce the limiting conditions. Similar to the $C_p(T-T_p)$ function, empirical parameters in equation 6 are analogous to the Arrhenius terms. ξ_1 and ξ_2 are the frequency parameters and carry the unit *1/℃*. ψ_1 and ψ_2 also have the same unit *1/℃*. B_1 and B_2 are the activation energy parameters and their units are the same as $R/\Delta E$ terms. Finally, all the numerator and denominator terms in equation 6 bear the unit *1/℃* rendering the function $\alpha_g(T-T_p)$ non-dimensionless as required.

The same least-square-error-fit procedure as discussed in Section 3 was adopted to map α_g values calculated using equation 2 based on Cp curves modeled using equation 3. Error minimization was achieved by employing equation 7:

$$\sum_{i=1}^{N}\left[\alpha_{g(ana)}-\alpha_{g(sig)}\right]^{2}\rightarrow 0 \tag{7}$$

The results for all the cases are shown in Figure 7. Good agreement was established with the analytically derived values of α_g using the C_p model, which was earlier found to agree well to the experimental data. The values of all the empirical constants are tabulated in Table 2. It can be observed from Table 2 that for the no-salt case, ψ_1 term was not essential. This implied that parameter ψ_1 was associated with the salt-out effects of NaCl. Thus, the same conclusion is reached as before that with the addition of salt, an additional mechanism is involved in the gelation process. Similar to the C_p model (Table 1), no clear trend was observed for the sigmoid curves constants for different salt concentrations.

An attempt was made to estimate the sol-gel activation energy parameters for the degree of gelation ($\Delta E\alpha_g$) by correlating B_1 and B_2 with $R/\Delta E$ terms. The calculated $\Delta E\alpha_{g1}$ and $\Delta E\alpha_{g2}$ values, which are based on the normalized energy represented by α_g, are shown in the last two rows of Table 2. These energy parameters are the process-specific remainders obtained after eliminating the effects of the process-independent universal gas constant. Thus, they relate more directly to the gelation process and the mechanism of sol-gel transformation.

6.0 Conclusions

A two-bell shaped model was developed for simulating the C_p curves defining the heat absorption during gelation of MC in the presence of NaCl additives. The import of various constants in terms of gelation kinetics was identified. The formulation worked well and could describe the MC gelation with different % of NaCl. Out of the two bell-shaped curves, which upon superimposing described the C_p variations with temperature, the dominant curve always mapped most of the experimental data and was designated as the primary curve. It appeared that the energy described by the curve was utilized mainly for the movement of MC macromolecules and their hydrophobic association leading to a gel network. The secondary curve, which always accounted for a small amount of energy, however, was necessary in order to describe accurately the left and right hand shoulders of the curve. This appeared to represent the energy utilized in the ionic interaction of salt with water and its effects during the stabilization of the gel.

A sigmoidal model with the appropriate units for each terms was formulated to describe the degree of gelation, α_g, for all cases. The correlation between the values derived using the C_p curves and the sigmoidal model was excellent. All α_g curves had approximately the same slope, except at the beginning and towards the end of gelation. This implied that the rate of gelation was not affected by the presence of NaCl during the phase when the movement of MC chains was a dominant activity.

References

1. Peppas NA, Bures P, Leobandung W, Ichikawa H, Hydrogels in pharmaceutical formulations - review article, European Journal of Pharmaceutics and Biopharmaceutics 2000; 50: 27-46.

2. Jeong B, Kim SW, Bae YH, Thermosensitive sol-gel reversible hydrogels, Advanced Drug Delivery Reviews 2000; 54 (1): 37-51.

3. Liu W, Zhang B, Lu WW, Li X, Zhu D, Yao KD, Wang Q, Zhao C, Wang C, A rapid temperature-responsive sol-gel reversible poly(N-isopylacrylamide)-g-methylcellulose copolymer hydrogel, Biomaterials 2004; 25: 3005-3012.

4. Lee WF, Chiu RJ, Thermoreversible Hydrogels XVI: Synthesis and swelling behaviours of [N-Isopropylacrylamide-co-trimethyl acrylamidopropyl ammonium iodide-co-3-dimethyl (methacryloxyethyl) ammonium propane sulfonate] copolymeric hydrogels in aqueous salt solution, Journal of Polymer research 2002; 9: 141-149.

5. Sarkar N, Walker LC, Hydration – dehydration properties of methylcellulose and hydroxypropylmethylcellulose, Carbohydrate Polymers 1995; 27: 177-185.

6. Desbrieres J, Hirrien M, Rinaudo M, A calorimetric study of methylcellulose gelation, Carbohydrate Polymers 1998; 37: 145-152.

7. Ford JL, Thermal analysis of hydropropylmethylcellulose and methylcellulose: powders, gels and matrix tablets, International Journal of Pharmaceutics 1999; 179: 209-228.

8. Kobayashi K, Huang C, Lodge TP, Thermoreversible gelation of aqueous methylcellulose solutions, Macromolecules 1999; 32: 7070-7077.

9. Joshi SC, Lam YC and Li L, Development of a gelation model for methyl cellulose hydrogels, Proceedings, ANTEC 2004 conference, May 16-20, 2004, Chicago, Illinois, USA, 2479-2483.

10. Joshi SC, Lam YC and Li L, Temperature dependent sol-gel transformation for methyl cellulose hydrogels and its modelling, Journal of Sol-gel transitions (under review).

11. Rosiak JM and Yoshii F, Hydrogels and their medical applications, Nuclear Instruments and Methods in Physics Research B 1999; 151: 56-64.

12. Li L, Shan H, Yue CY, Lam YC, Tam KC, Hu X, Thermally induced association and dissociation of methyl cellulose in aqueous solutions, Langmuir 2002; 18: 7291-7298.

13. Kundu PP, Kundu M, Effect of salts and surfactant and their doses on the gelation of extremely dilute solutions of methyl cellulose, Polymer 2001; 42: 2015-2020.

14. Xu Y, Wang C, Tam KC, Li L, Salt-assisted and salt-suppressed sol-gel transitions of methylcellulose in water, Langmuir 2004; 20: 646-652.

15. Xu YR, Li L, Zheng PJ, Lam YC, Hu X, Controllable gelation of methylcellulose by a salt mixture, *Langmuir 2004;* 20 (15): 6134-6138.

16. Lee SC, Cho YW and Park K, Control of thermogelation properties of hydrophobically-modified methylcellulose, Journal of Bioactive and Compatible Polymers 2005; 20 (1): 5-13.

17. Lee WI and Springer GS, Pultrusion of thermoplastics- a model, Journal of Composite

Materials 1991; 25:1632-1652.

18. Um MK, Daniel IM, Hwang BS, A study of cure kinetics by the use of dynamic differential scanning calorimetry, Composites Science and Technology 2002; 62: 29-40.

19. R. Chang, Chemistry, 8th edition, McGraw-Hill publications, 2005, p. 556.

20. Lee WI, Loos AC, Springer GS, Heat of reaction, degree of cure, and viscosity of Hercules 3501-6 resin, Journal of Composite Materials 1982; 16:510-520.

21. Ozawa T, Kinetics of non-isothermal crystallization, Polymer 1977; 12: 150-158.

22. Rutledge RG, Sigmoidal curve-fitting redefines quantitative real-time PCR with the prospective of developing automated high-throughput applications, Nucleic Acids Research 2004; 32(22), Oxford University Press, Published online.

23. DeVoe RD, de Souza JM and Ventura DF, Electrophysiological measurements of spectral sensitivities: a review, Brazilian Journal of Medical and Biological Research 1997; 30: 169-177.

List of Figures

1. Schematic illustration of temperature dependent sol-gel transformations for aqueous solution of MC. (Black DOTS represent water associated molecules. Dark LINES are the MC chains with short branches as methaxyl side groups. Hydrophobic associative bonds of these side groups are shown on a patterned whitish OVAL shapes.)
2. DSC curves for different NaCl concentrations in 0.03mM of MC solutions (scanning rate 1°/min).
3. Specific heat capacity and degree of gelation curves for MC hydrogel with NaCl (Single bell-shape model).
4. Specific heat capacity curves for the MC hydrogel with NaCl (two bell-shape model).
5. Total heat of gelation as a function of NaCl concetration.
6. Degree of gelation curves for MC gelation obtained using equations 2 and 3.
7. Plots for degree of gelation for MC hydrogels obtained using the sigmoidal model (equation 6).

List of Tables

1. The model constants for C_p curves (Equations 1 and 3)
2. The sigmoidal model constants for α_g curves (Equation 6) and the sol-gel activation energy parameters for MC gelation

Figure

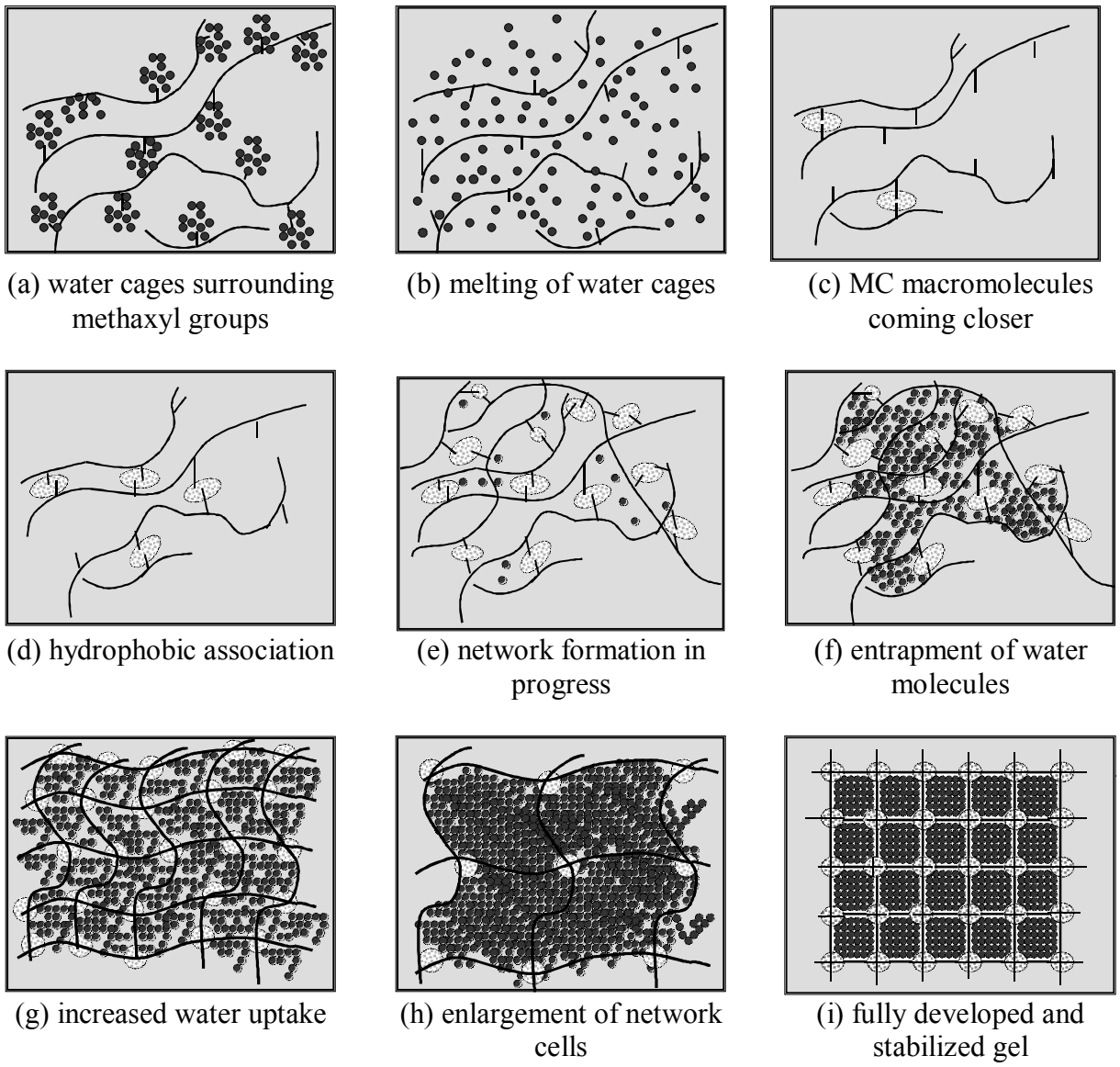

Figure 1: Schematic illustration of temperature dependent sol-gel transformations for aqueous solution of MC. (Black DOTS represent water associated molecules. Dark LINES are the MC chains with short branches as methaxyl side groups. Hydrophobic associative bonds of these side groups are shown on a patterned whitish OVAL shapes.)

Figure

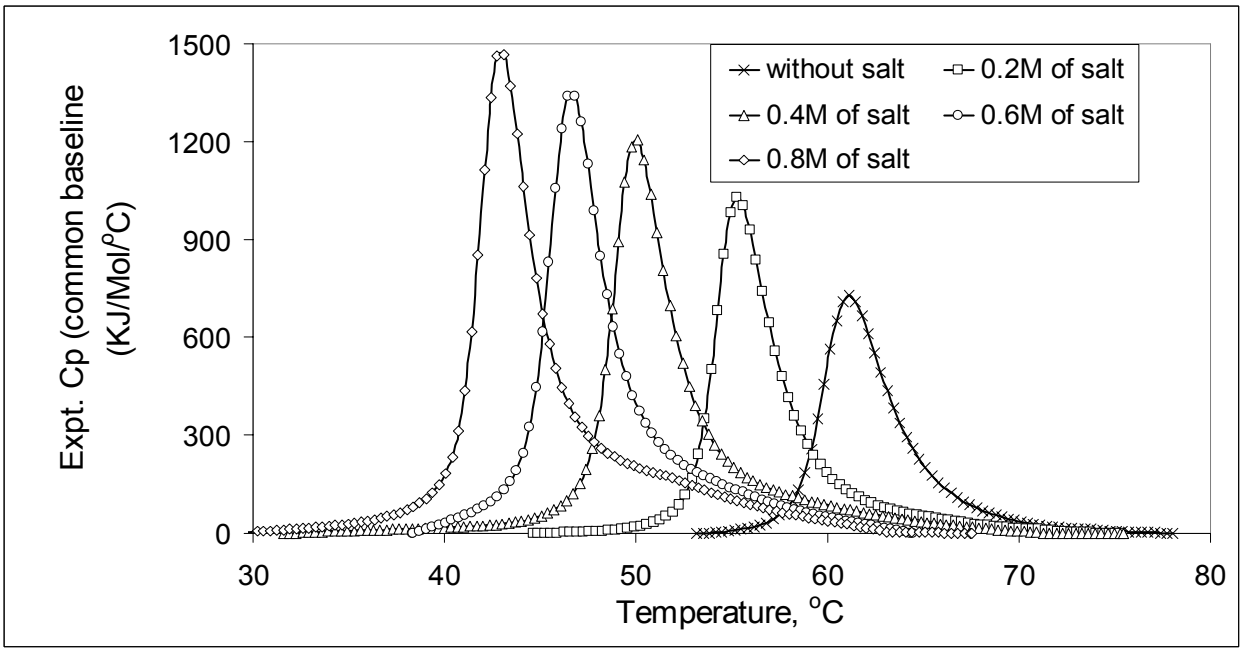

Figure 2: DSC curves for different NaCl concentrations in 0.03mM of MC solutions (scanning rate 1°/min).

Figure

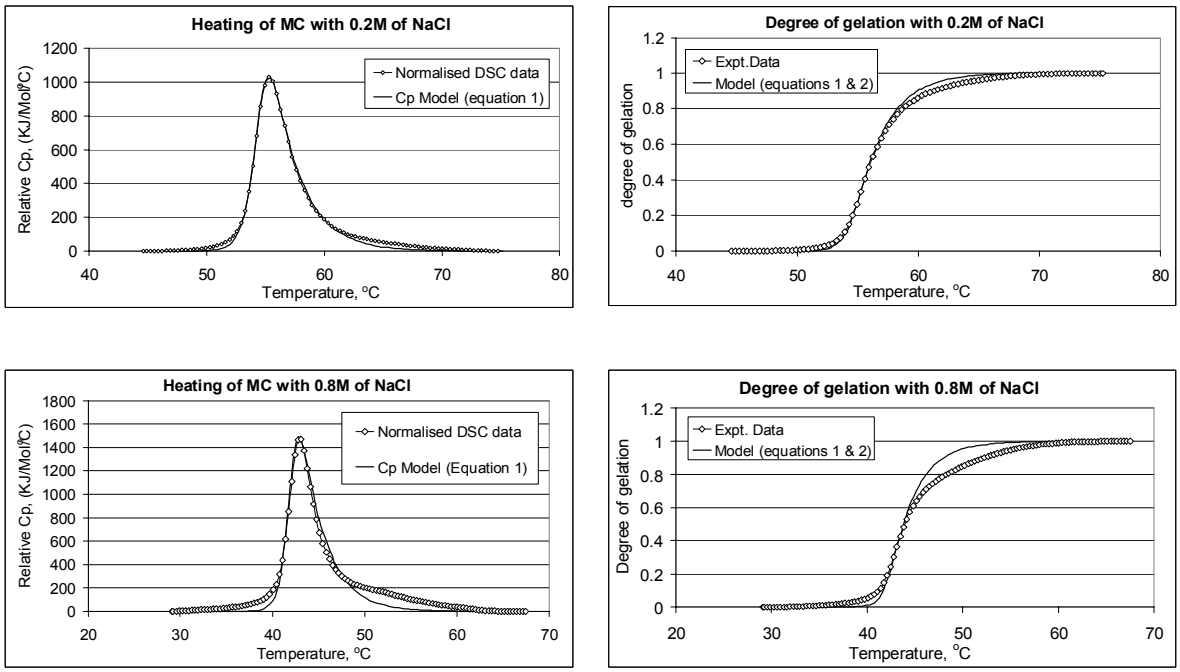

Figure 3: Specific heat capacity and degree of gelation curves for MC hydrogel with NaCl (Single bell-shape model).

Figure

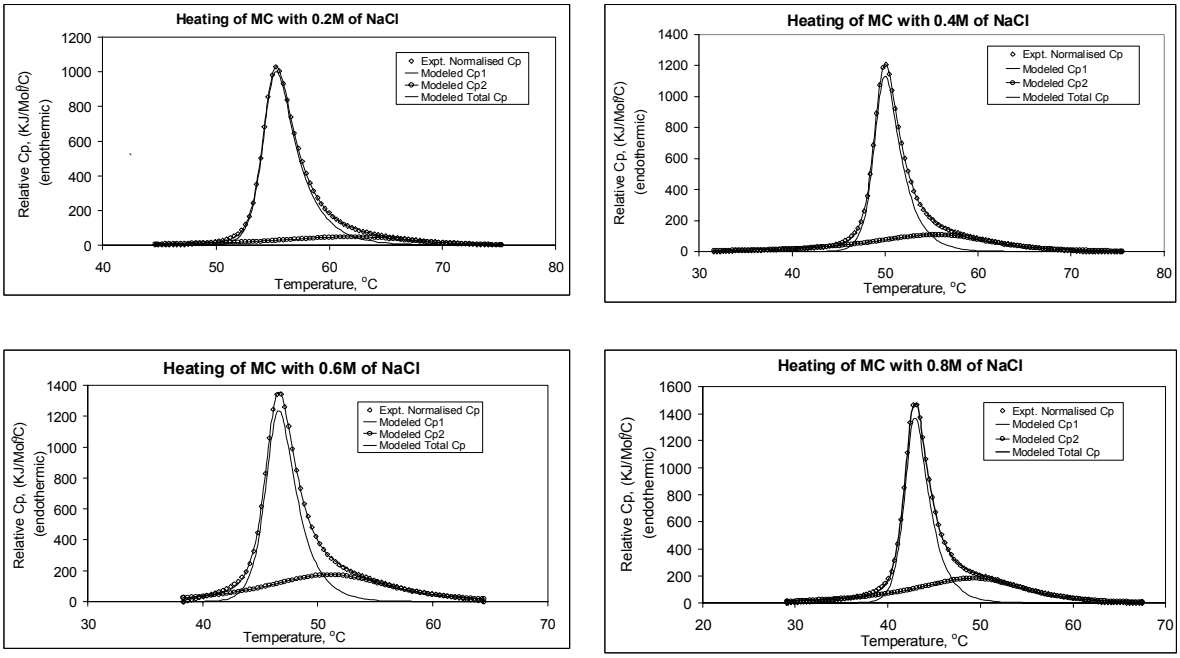

Figure 4: Specific heat capacity curves for the MC hydrogel with NaCl (two bell-shape model).

Figure

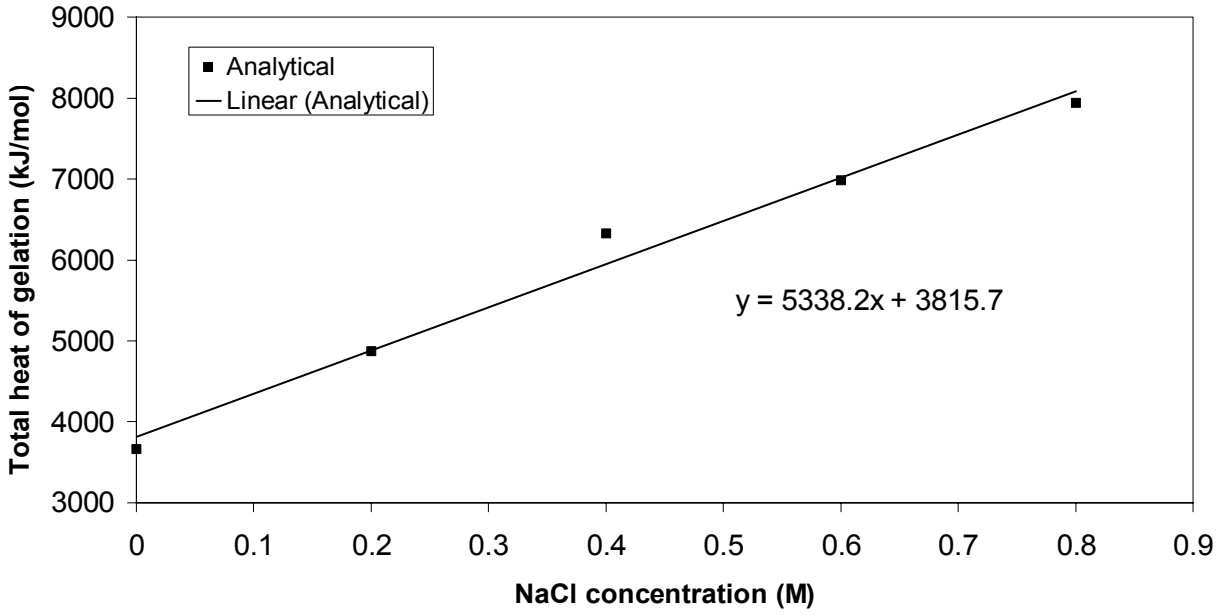

Figure 5: Total heat of gelation as a function of NaCl concetration.

Figure

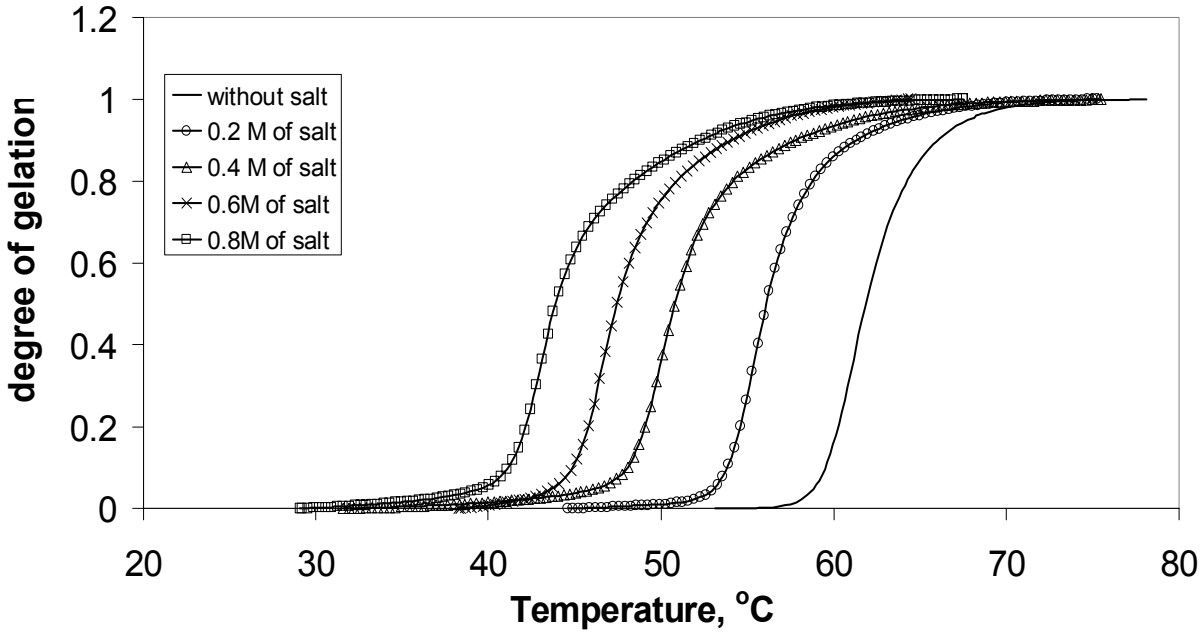

Figure 6: Degree of gelation curves for MC gelation obtained using equations 2 and 3.

Figure

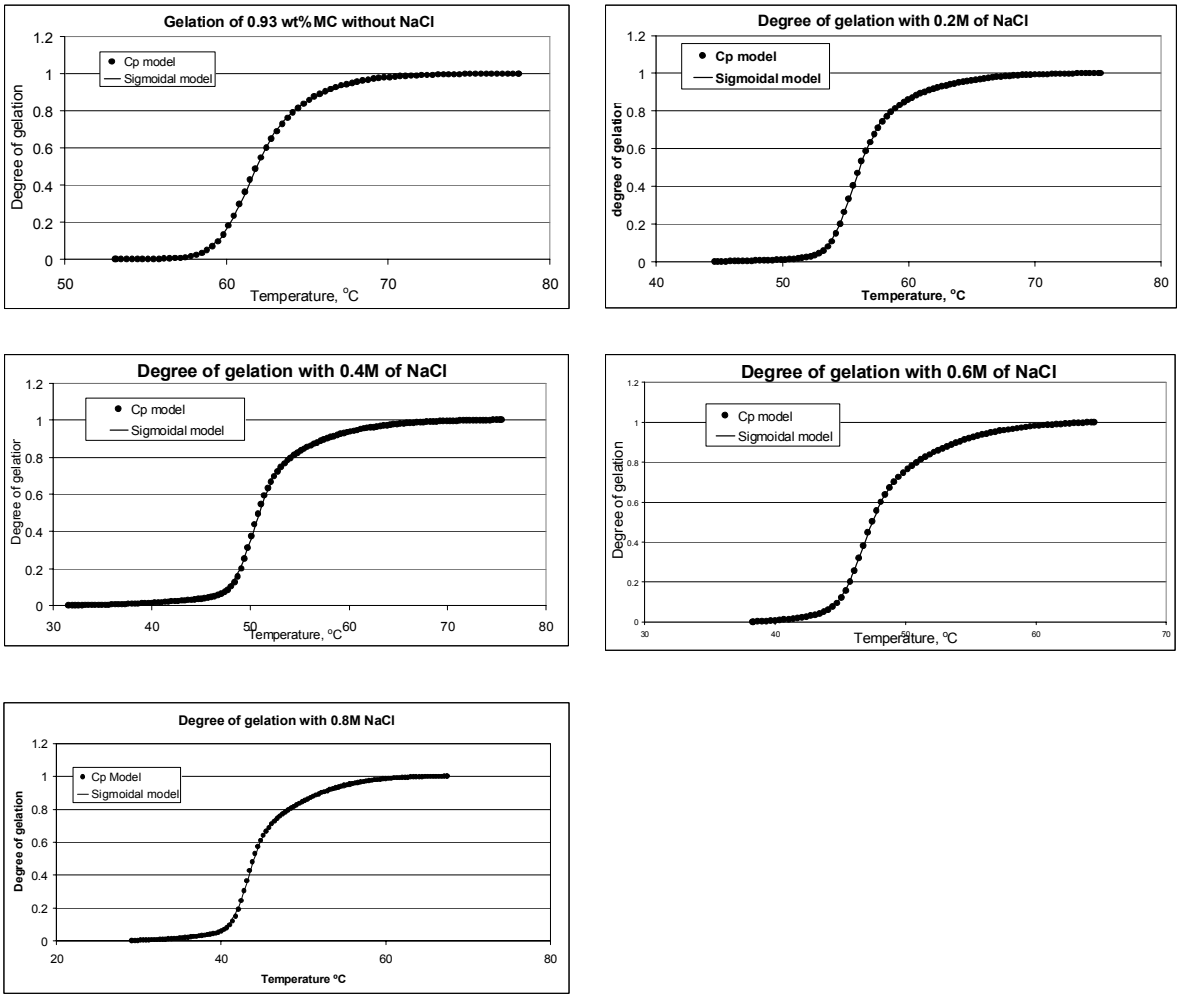

Figure 7: Plots for degree of gelation for MC hydrogels obtained using the sigmoidal model (equation 6).

Table

Table 1: The model constants for C_p curves (Equations 1 and 3)

Constants	NaCl concentration				
	0.0M (1)	0.2M (3)	0.4M (3)	0.6M (3)	0.8M (3)
λ_1 (1/ºC)	1.8985	1.9774	2.9376	0.0402	4.6263
λ_2 (1/ºC)	0.632	2.2097	1.3632	0.00952	0.3665
λ_3 (1/ºC)	-	0.0971	0.0737	0.3072	0.0975
λ_4 (1/ºC)	-	0.1256	0.1262	0.8208	1.435
C_1 (1/ºC)	0.392	0.4882	0.5532	0.6232	0.6091
C_2 (1/ºC)	1.144	1.3319	1.2516	1.2024	1.2837
C_3 (1/ºC)	-	0.2961	0.2228	0.2292	0.2397
C_4 (1/ºC)	-	0.1428	0.1448	0.1998	0.1560
C_{pv1} (kJ/mol/ºC)	-	874.2	1134.47	1164.78	1054.95
C_{pv2} (kJ/mol/ºC)	-	47.074	108.539	160.079	115.996
T_{p1} (ºC)	61.14	54.71	49.96	47.04	43.88
T_{p2} (ºC)	-	63.11	55.18	49.07	43.53

Table 2: The sigmoidal model constants for α_g curves (Equation 6) and the sol-gel activation energy parameters for MC gelation

Constants	NaCl concentration				
	0.0M	0.2M	0.4M	0.6M	0.8M
ψ_1 (1/ºC)	-	0.0205	0.0624	0.0622	0.0702
ψ_2 (1/ºC)	0.7058	0.9062	0.8654	0.5988	0.7483
ξ_1 (1/ºC)	1.5502	1.5366	1.3178	1.5369	1.3668
ξ_2 (1/ºC)	0.7045	0.7496	0.7303	0.7776	0.7319
B_1 (1/ºC)	0.9122	0.9706	0.8125	0.9612	0.8772
B_2 (1/ºC)	0.9593	1.007	0.8356	0.9999	0.9024
$\Delta E\alpha_{g1}$ (J/mol)	9.11	8.56	10.23	8.65	9.48
$\Delta E\alpha_{g2}$ (J/mol)	8.67	8.26	9.95	8.31	9.21